

## Tuned LNA for RFICs using *boot-strapped* inductor

Fleana Albertoni, Luca Fanucci\*, Bruno Neri, Enrico Sentieri

Università di Pisa, Dipartimento di Ingegneria dell'Informazione, Pisa, I-56122, Italy

\* C.S. Metodi e Dispositivi per Radiotrasmissioni, Consiglio Nazionale delle Ricerche, Pisa, Italy

**Abstract** — In this paper, the principle of operation of a new type of active inductor and its application to a tuned LNA are described. The design is optimized at 1.8 GHz. An integrated transformer in connection with a current amplifier realizes a “boot-strapped” inductor with a  $L \times Q$  factor never obtained before at this frequency. This way a selective LNA with a 60 MHz bandwidth, corresponding to a  $Q$  of 30, was designed. The circuit exhibits a matched noise figure of 1.8 dB with 25.5 dB transducer power gain while dissipating 20.7 mW from a 3 V power supply.

### I. INTRODUCTION

The realization of high quality factor ( $Q$ ) integrated inductors is one of the most intriguing problems in the design of RF front-ends for integrated transceivers. In a previous work [1] the results which can be obtained in terms of inductance ( $L$ ) and  $Q$  values by using a novel circuit topology have been described. This solution, whose basic principles will be briefly summarized in Section II, allows to obtain very high value of the  $Q \times L$  factor. Other solutions, based on the utilization of active devices, have been proposed in the past to improve the  $Q$  factor with respect to that of passive spiral inductors [2-3]. However, none of these solutions is capable to increase the effective  $L$  value which, in silicon integrated devices, is normally limited to a few nanoHenry at frequencies of about 2 GHz. The approach proposed in this paper allows to improve both the effective values of  $L$  and  $Q$ , almost up to a factor of 10, while keeping practically constant the occupied silicon area. As it will be shown in Sections III and IV this solution can be advantageously used to design tuned Low Noise Amplifiers (LNA) capable, for instance, of attenuate the image frequency by 25 dB @ 200 MHz of intermediate frequency.

### II. BOOT-STRAPPED INDUCTOR

In order to increase the  $Q$ -factor of integrated inductors (defined as the ratio between the imaginary part and the real part of its impedance) many techniques have been presented [4, 5]. Nevertheless it is not simple to obtain  $Q$ -factors greater than 8 for inductors of few nH. Indeed, achievable  $Q$  values decrease as the inductor value rises.

An improvement of  $Q$  can be obtained by using active circuits to compensate for the losses of the integrated inductor [6]. This method, anyway, does not provide any increase of the inductance value and it may lead to instability. Moreover, the robustness versus the process parameter tolerances, and, consequently, their practical implementation, has not been demonstrated yet.

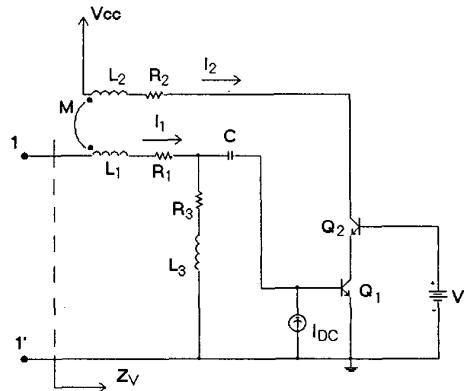


Fig. 1: Boot-strapped inductor

Here, we propose a solution based on the circuit depicted in Fig. 1. This circuit exploits the magnetic coupling between two spiral inductors ( $L_1$  and  $L_2$  in Fig. 1) to increase the inductance value seen at the input terminals 1-1'. The inductor  $L_3$ , its parasitic series resistance  $R_3$  and the base-emitter capacitance of  $Q_1$  realize an LRC filter. If the value of  $L_3$  is chosen in such a way to resonate with the input capacitance of  $Q_1$ , then the current through  $L_1$  is in phase with the base-to-emitter voltage of  $Q_1$ . In this case, the currents  $I_1$  and  $I_2$  are in phase, provided that the equivalent transconductance  $g_m^*$  of the cascode stage is a real value. Because of the magnetic coupling, the voltage drop on  $L_1$  is increased by the factor  $\omega M g_m^* r_\pi I_1$ , where  $\omega$  is the operating frequency,  $M$  is the mutual inductance between  $L_1$  and  $L_2$  and  $r_\pi$  is the base-to-emitter differential resistance of  $Q_1$ . In this case the value of the equivalent inductance seen at the terminals 1-1' would be increased

by a factor  $Mg_m^* r_\pi$ . More in general the input impedance seen at terminals 1-1' ( $Z_V$ ) is expressed by the following formula:

$$Z_V = [R_1 + r_\pi - \omega \cdot M \cdot g_m^* \cdot r_\pi \cdot \sin \varphi] + j\omega \cdot [L_1 + M \cdot g_m^* \cdot r_\pi \cdot \cos \varphi] \quad (1)$$

where  $R_1$  is the parasitic series resistance of  $L_1$  and  $\varphi$  is the angle between  $I_1$  and  $I_2$ . This way the equivalent inductance value is increased by a factor  $Mg_m^* r_\pi \cos \varphi$ , whereas the real part is decreased by  $\omega Mg_m^* r_\pi \sin \varphi - r_\pi$ . By changing  $\varphi$ , which depends on the intrinsic capacitances of  $Q_1$  and  $Q_2$ , different values of the effective inductance can be obtained. This task can be accomplished by changing the bias current of  $Q_1$  and the base voltage of  $Q_2$  [1].

In Fig. 2 the performances of actual integrated inductors in Si-Ge technology [7], in terms of  $Q$  and  $L$ , are compared with the typical performance which has been obtained by using the new circuit block depicted in Fig. 1, which has been called "boot-strapped" inductor.

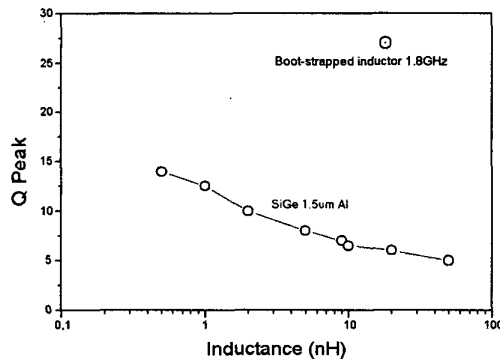


Fig. 2:  $Q$  versus  $L$  for SiGe spiral inductors [7]. Circle with dot represents a typical result obtained by using the boot-strapped inductor described in this paper.

### III. TUNED LNA

The LNA is the most critical stage as far as the overall Noise Figure (NF) of the receiver is concerned. NF values as low as 2 dB are sometimes required in modern wireless terminals. In superheterodyne architecture, which is, at present, the most widely adopted for this type of application, the LNA should perform also another task: it should introduce a sufficiently large attenuation of the image frequency. Indeed, presently realizable image rejection mixers are unable to obtain an image frequency rejection larger than 40 dB, whereas some applications, for

instance GSM standard, require overall attenuation as high as 70 dB. To this end tuned amplifiers using high  $Q$  monolithic external filters (ceramic or surface acoustic wave types) are required. The drawback of this solution consists of the need of supplemental pins and external components which are more costly and introduce noise and attenuation also in the pass band. The realization of entirely integrated tuned amplifiers, in the GHz range, represents a very stimulating target for RF IC designers. Several solutions have been proposed in literature using active inductors, realized by means of a gyrator [8, 9] or by shunting passive spiral inductors with an active bipole presenting a negative resistance [10]. In all of these cases, the operating frequency is lower or equal to 1 GHz and the dissipated power and/or the noise figure are quite high. Moreover the possibility of compensating for the effect of the silicon process tolerances and of the temperature variations has not been demonstrated. A comparison between their performances and those obtained by using boot-strapped inductors is presented at the end of Section IV.

The circuit scheme of a tuned LNA using this new type of active inductor is depicted in Fig. 3. It is based on a transconductance stage to drive the current into a shunt LRC resonant filter, where  $R$  and  $\omega L$  are the real and the imaginary part of  $Z_V$  respectively, which is realized following the boot-strapped inductor approach described in Section II.

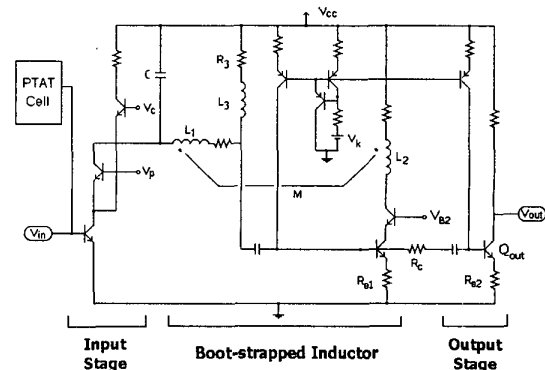


Fig. 3: Schematic of the selective LNA.

The input stage sets the noise figure of the amplifier, while the effective inductance value and the quality factor  $Q$  of the boot-strapped inductor, can be controlled by means of  $V_K$  and  $V_{B2}$ . The variable component of the current through  $L_1$  has a maximum at the frequency  $f_0$  at which the LRC filter resonates. The output stage is a

current mirror which transfers this current, multiplied by the current gain of  $Q_{OUT}$ , to the external load. A PTAT (Proportional To Absolute Temperature) cell to bias the input stage is used in order to counteract temperature variations effects on LNA voltage gain ( $A_v$ ). As it will be detailed in Section IV, the voltage  $V_c$ , driven by a signal proportional to the LNA output power level could be used to expand the LNA input dynamic range.

The amplifier is designed on ST's HSB2 bipolar process (a  $0.4 \mu\text{m}$  emitter width trench oxide isolated bipolar process with three layers of metal and  $20 \text{ GHz}$  bjt's cut off frequency). The integrated transformer is made up by two identical coupled inductors, the first one in metal 3, the second one in metal 2: square shaped,  $225 \mu\text{m}$  per side, three turns each, metal track  $10 \mu\text{m}$  wide,  $10 \mu\text{m}$  spacing between adjacent metal tracks. The inductor  $L_3$  is also square shaped,  $120 \mu\text{m}$  per side, 2 turns in metal 3 ( $10 \mu\text{m}$  wide with  $8 \mu\text{m}$  spacing) in series with 3 turns in metal 2 ( $8 \mu\text{m}$  wide with  $8 \mu\text{m}$  spacing). A thick grid of trenches underneath the inductors has been used to reduce the induced currents in the substrate, so allowing a higher value of the Q-factor. The layout of the complete LNA is shown in Fig. 4 (where trenches underneath inductors were removed for a sake of clarity): the overall chip size is  $0.52 \text{ mm}^2$  and it is mainly due to the distance (nearly  $400 \mu\text{m}$ ) between the transformer and the passive inductor, needed to achieve a sufficient magnetic de-coupling between the two structures [11].

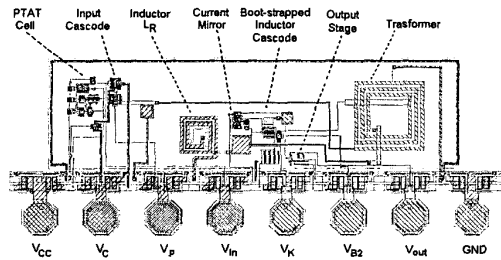


Fig. 4: Layout of the LNA.

#### IV. SIMULATION AND RESULTS

The design of the amplifier has been preceded by an accurate electromagnetic simulation of the transformer and the passive inductor, as described in [12]. Then the extracted Z parameters of the equivalent circuit of the transformer were input to the Mentor Graphics ELDO<sup>TM</sup> simulator to obtain the frequency response of the overall circuit. The transducer power gain ( $G_T$ ), defined as the ratio between the power supplied to the load and the available power at the input, is depicted in Fig. 5 versus

frequency. These data are based on post-layout simulations for the case of minimum NF matching. It reaches a peak value of  $25.5 \text{ dB}$  at  $1.8 \text{ GHz}$  for a band-width of  $60 \text{ MHz}$ , which results in a quality factor of 30. This corresponds to an image-reject filtering of  $18.8 \text{ dB}$  and  $25 \text{ dB}$  for a  $100 \text{ MHz}$  and  $200 \text{ MHz}$  intermediate frequency respectively.

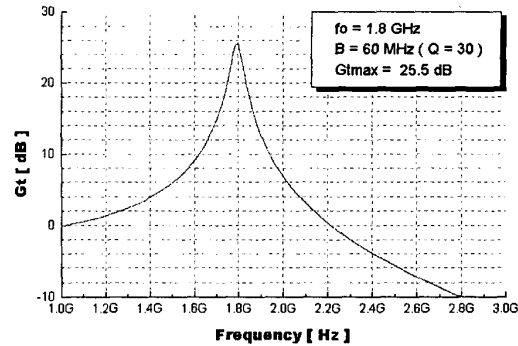


Fig. 5: LNA transducer gain based on post-layout simulations.

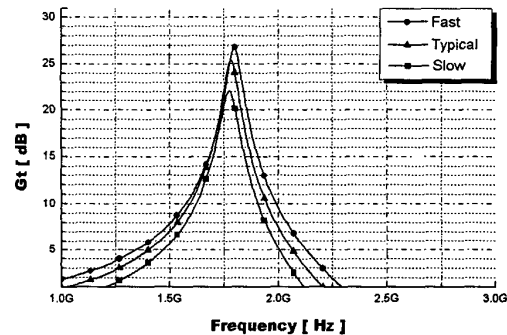


Fig. 6: LNA transducer gain variation due to silicon process tolerances based on post-layout simulations (slow, typical and fast process models).

One of the limiting factor in the utilization of highly selective integrated circuit is the reproducibility of the results which is affected mainly by the spreading of the parameters of the active devices. To this end the effect of the process tolerances have been simulated by using typical, as well as slow and fast models for bipolar transistors. In Fig. 6 it is shown as this effect can be quite completely compensated by using the two control voltages  $V_{B2}$  and  $V_K$ . Particularly, the variation of the resonance frequency and of the bandwidth can be kept below  $0.3\%$  and  $5\%$  respectively, by acting on  $V_{B2}$  and  $V_K$  and below  $0.8\%$  and  $5\%$  by using only  $V_K$ .

By using the PTAT cell of Fig. 3, which determines a negligible silicon area increase, the LNA voltage gain due to temperature variations in the range [0°C-80°C] is kept below 6.5%.

The amplifier results unconditionally stable at least up to 5 GHz (the upper limit used for circuit analysis). The minimum NF of the LNA, obtained through proper impedance matching with the input signal source, is 1.8 dB and it is mainly due to the input stage according to the Friis formula.

Another very critical characteristic for wireless applications is the dynamic range, namely the 1 dB compression point ( $CP_{1dB}$ ). The proposed circuit is characterized by a  $CP_{1dB}$  of -50 dBm. By varying the control voltage  $V_C$ , in the range [2.6 V - 2.9 V], it is possible to increase the input dynamic range up to -20 dBm without any modification of the resonance frequency and of the bandwidth but at the expenses of a voltage gain reduction.

Finally in Table 1 a comparison among the main characteristics of silicon integrated tuned LNA presented in literature and the solution described in this paper is shown. To be noted that none of these circuits have been optimized for an operating frequency higher than 1 GHz. The ones with similar and/or higher selectivity than ours exhibit a NF from 2.5 to 4.2 dB higher and a power consumption greater than almost 3 to 4 times. Moreover, the proposed amplifier outperforms the others in terms of voltage gain.

TABLE I  
PROPOSED LNAs COMPARISON

	Technol.	$A_V$ [dB]	NF [dB]	$f_0$ [GHz]	$P_d$ [mW]	Q
[8]	CMOS	17	6	0.9	78	30
[9]	BiCMOS	18	4.3	1	57	56
[10]	CMOS	20	3.6	1	14	5
OUR	BJT	22.5	1.8	1.8	20.7	30

## V. CONCLUSION

The design and post layout simulation results of a tuned LNA have been presented. By using a new type of active inductor a Q value of 30 at 1.8 GHz has been obtained, while keeping the NF very close to its minimum value compatible with the used technology. The robustness of the design versus temperature variations and silicon process tolerances have been demonstrated. The integration of such an LNA with a novel image rejection

mixer [13] is currently pursued targeting to an integrated RF front-end capable of attenuating by 70 dB the image frequency without external components.

## ACKNOWLEDGEMENT

The financial support of the Italian National Research Council through the Finalized Project "Materials and Devices for Solid State Electronics II" is gratefully acknowledged.

## REFERENCES

- [1] G. D'Angelo, L. Fanucci, A. Monorchio, A. Monterastelli, and B. Neri, "High Quality Active Inductors", *IEEE Electronic Letters*, N. 20, pp. 1727-1728, September 1999.
- [2] H. Hayashi, M. Muraguchi, Y. Umeda, and T. Enoki, "A novel loss compensation technique for high-Q broad-band active inductors", *IEEE Microwave and Millimeter wave Monolithic Circuits Symposium Digest*, pp.103-106, 1996.
- [3] Yei Li, B.L.Ooi, Q.J.Xu, and P.S.Kooi, "High Q active inductor with loss compensation by feedback network", *IEEE Electronic Letters*, N. 35, pp. 1328-1329, August 1999.
- [4] J. N. Burghartz, K. A. Jenkins, M. Soyuer: "Multilevel Spiral Inductors using VLSI Interconnect Technology", *IEEE Electron Device Letters*, Vol. 17, pp. 428-431, September 1996.
- [5] F. Mernyei, F. Darrer, M. Pardoen, A. Sibrai: "Reducing The Substrate Losses for RF Integrated Inductors", *IEEE Microwave and Guided Wave Letters*, Vol. 8, pp. 300-301, September 1998.
- [6] W. B. Kuhn, N.K. Yanduru, and A. S. Wyszynski: "Q-Enhanced LC Bandpass Filters for Integrated Wireless Applications", *IEEE Trans. MTT*, Vol. 46, pp. 2577-2586, December 1998.
- [7] L. E. Larson, "Integrated circuit technology options for RF IC's - Present status and future directions", *IEEE Journal of Solid State Circuits*, vol.33, p.387-399, March 1998.
- [8] C. Y. Wu, and S. Y. Hsiao, "The Design of a 3-V 900-MHz CMOS Bandpass Amplifier", *IEEE Journal of Solid-State Circuits*, vol. 32, no. 2, pp. 159-167, February 1997.
- [9] A. Thanachayanont, A. Payne: "A 3-V RF CMOS Bandpass Amplifier using an Active Inductor", *Proc IEEE Int. Symp. Circuits and Systems*, vol. 1, pp. 440-443, May-June 1998, New York, USA.
- [10] W. Zhuo, J. Pineda de Gyvez, E. Sánchez-Sinencio: "Programmable Low Noise Amplifier with Active - inductor Load", *Proc IEEE Int. Symp. Circuits and Systems*, vol. 4, pp. 365-368, May-June 1998, New York, USA.
- [11] Y. Koutsoyannopoulos, Y. Papanamos, S. Bantas, C. Alemanni: "Novel Si Integrated Inductor and Transformer Structures for RF IC Design", *Proc IEEE Int. Symp. Circ. and Syst.*, vol. II, pp. 61-64, May 1999, Orlando, Florida.
- [12] G. D'Angelo, A. Granchi, A. Monorchio, B. Neri: "Design and Simulation of Active Spiral Inductors for RF Integrated Circuits", *Proc of IEEE APS International Symposium*, pp. 1836-1839, July 1999, Orlando, Florida.
- [13] G. Palmisano et al. "Integrated RF Image Rejection Mixer", *unpublished*.